High-frequency corrections to ground-based searches for long-duration gravitational waves

M Rakhmanov[1], J D Romano[1,2] and J T Whelan[3]

[1] University of Texas at Brownsville, Brownsville, Texas, 78520, USA
[2] Cardiff University, Cardiff CF24 3AA, Wales, UK
[3] Max-Planck-Institut für Gravitationsphysik (Albert-Einstein-Institut), Potsdam, GDR

E-mail: malik@phys.utb.edu, joe@phys.utb.edu, john.whelan@aei.mpg.de

Abstract. Most gravitational-wave searches with ground-based interferometers have been conducted in the long-wavelength approximation, where the change in the gravitational wave during a round-trip of the laser light is neglected. The nominal correction to the long-wavelength approximation is at the few-percent level for frequencies of order 1 kHz and 4-km-long arms like LIGO. Here we estimate the effect of using the long-wavelength approximation on two of the standard ground-based searches: an isotropic stochastic gravitational-wave background, and a periodic gravitational-wave signal emitted by a known pulsar. We find that for frequencies of order 1 kHz, the effect of corrections to the long-wavelength approximation are much less than 1% for searches performed so far. However, the correction to the planned LIGO Hanford-Livingston cross-correlation search for an isotropic stochastic background near 1 kHz is at the 4%-level. In addition, the presence of Fabry-Perot cavities in the interferometer arms gives us another frequency band to search for gravitational waves—at the free-spectral range of the Fabry-Perot cavities (37.5 kHz for LIGO)—where the exact detector response is required.

PACS numbers: 04.80.Nn, 95.55.Ym

1. Introduction

Searches for gravitational waves with ground-based interferometers such as LIGO [1], Virgo [2], and GEO-600 [3] have been typically carried out in the long-wavelength approximation, where the change in the gravitational wave during a round-trip of the laser light is neglected. This amounts to ignoring terms of order L/λ, where L is the arm length of the interferometer and λ is the wavelength of the gravitational wave. For the LIGO detectors ($L = 4$ km) near the upper end of its sensitivity band (few kHz), the nominal correction is of order 5-10%. Since the largest uncertainty for current gravitational-wave searches is at the 5% level (from calibration uncertainties), it is important to assess the systematic errors that the long-wavelength approximation may introduce.

In this paper, we estimate the effect of using the long-wavelength approximation on two standard ground-based searches for long-lived gravitational-wave signals: an isotropic stochastic gravitational-wave background, and a periodic gravitational-wave signal emitted by a known pulsar. (The formalism described here can be extended

to other searches—e.g., for gravitational-wave bursts.) In Secs. 2 and 3, we derive expressions for the response of a detector to a plane-polarised gravitational wave. We give exact expressions and expressions valid in the long-wavelength limit, for both a simple Michelson interferometer and an interferometer with Fabry-Perot arm cavities. (*First-order* corrections to the long-wavelength approximation for a simple Michelson interferometer were considered in a recent paper [4].) In Secs. 4 and 5, we describe how the standard searches for isotropic stochastic gravitational-wave backgrounds and periodic gravitational waves are affected by the long-wavelength approximation. Finally, in Sec. 6, we summarise our results and briefly describe an application where the exact expressions for the detector response are definitely needed—a new search at the free-spectral range (FSR) of the LIGO detectors.

2. Antenna pattern functions (static limit)

In the transverse-traceless gauge, a plane-polarised gravitational wave coming from direction $\hat{n}$ is given by

$$h_{ij}(t,\vec{x}) = h_+(t,\vec{x})e^+_{ij}(\hat{n}) + h_\times(t,\vec{x})e^\times_{ij}(\hat{n})\,, \tag{1}$$

where $h_{+,\times}(t,\vec{x}) = h_{+,\times}(t+\vec{x}\cdot\hat{n}/c)$, and the polarization tensors are defined by

$$e^+_{ij}(\hat{n}) = \ell_i\ell_j - m_i m_j, \tag{2}$$

$$e^\times_{ij}(\hat{n}) = \ell_i m_j + m_i\ell_j\,. \tag{3}$$

Here $\hat{\ell}$, $\hat{m}$ are chosen so that $(\hat{\ell},\hat{m},\hat{n})$ is a right-handed orthonormal basis. (There is rotatational freedom associated with the choice of $\hat{\ell}$, $\hat{m}$.)

Consider a simple Michelson interferometer with arms aligned along the unit vectors $\hat{a}$ and $\hat{b}$. In the long-wavelength limit ($L/\lambda \to 0$), a gravitational wave produces a signal in the interferometer [5]:

$$V(t) = \frac{1}{2}(a^i a^j - b^i b^j)h_{ij}(t,\vec{0}) \equiv F_+(\hat{n})h_+(t) + F_\times(\hat{n})h_\times(t), \tag{4}$$

where $F_A(\hat{n})$ are the *static* (zero frequency) interferometer responses to the two independent polarisations ($A = +,\times$) of the gravitational wave,

$$F_A(\hat{n}) = \frac{1}{2}\,(a^i a^j - b^i b^j)e^A_{ij}(\hat{n}), \tag{5}$$

also known as *antenna pattern functions*. Figure 1 is a plot of the magnitude of the static antenna pattern functions $F_A(\hat{n})$ for $\hat{a} = \hat{x}$, $\hat{b} = \hat{y}$.

3. Detector response to gravitational waves (exact formulae)

Taking into account the finite size of the detectors leads to *frequency-dependent* detector responses, as shown for example in early calculations for LIGO [6, 7, 8] and LISA [9, 10, 11]. Here we briefly derive the main formulae following [8]. The fundamental ingredient is the calculation of the round-trip light-travel time down an arm of the interferometer in the presence of a gravitational wave.

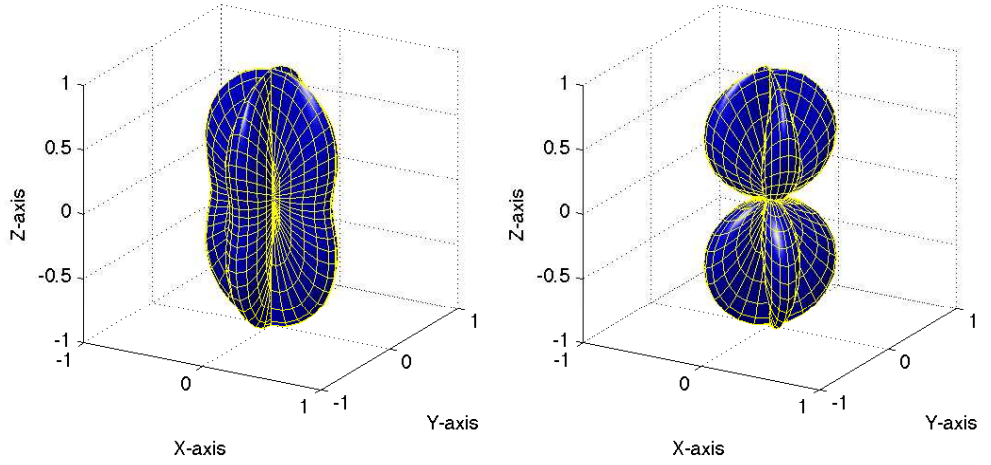

Figure 1. Static antenna pattern functions $|F_+(\hat{n})|$ [left panel] and $|F_\times(\hat{n})|$ [right panel].

3.1. Photon round-trip time

The interval for a photon propagating in the gravitational-wave background is

$$ds^2 = -c^2dt^2 + [\delta_{ij} + h_{ij}(t,\vec{x})]\, dx^i dx^j = 0\,. \tag{6}$$

Consider a round-trip for photons launched along an arm $\hat{a}$ of a gravitational-wave detector. The unperturbed trajectory for photons is $x^i = x_0^i \pm a^i\xi$, where ξ is the parameter along the photon trajectory: $0 \le \xi \le L$. Substituting this trajectory in (6) and solving for t, we obtain

$$c(t - t_0) = \int_0^\xi \left(1 + h_{ij}\, a^i a^j\right)^{1/2} d\xi'\,. \tag{7}$$

Let T be the nominal (unperturbed) photon transit time: $T \equiv L/c$. In the presence of a gravitational wave, the transit time will slightly deviate from its nominal value: $T_{1,2} = T + \delta T_{1,2}$. For forward propagation

$$\delta T_1(t) = \frac{1}{2c} a^i a^j \int_0^L h_{ij}\left(t_0 + \frac{\xi}{c} + \frac{\hat{n}\cdot\hat{a}}{c}\xi\right) d\xi\,, \tag{8}$$

where t_0 is the starting time for the photon propagation which can be approximated by $t_0 = t - T$. For the return trip,

$$\delta T_2(t) = \frac{1}{2c} a^i a^j \int_0^L h_{ij}\left(t_0 + \frac{L-\xi}{c} + \frac{\hat{n}\cdot\hat{a}}{c}\xi\right) d\xi\,. \tag{9}$$

Here too t_0 can be approximated by $t_0 = t - T$. The total time lag during the round trip is

$$\delta T(t) = \delta T_1[t - T_2(t)] + \delta T_2(t)\,, \tag{10}$$

where $T_2(t)$ can be replaced with T to first order in h. Taking the Fourier transform of this quantity we obtain

$$\frac{\delta\tilde{T}(f)}{T} = D(\hat{a}, f) a^i a^j \tilde{h}_{ij}(f)\,, \tag{11}$$

where $D(\hat{a}, f)$ is the corresponding transfer function

$$D(\hat{a}, f) = \frac{e^{-i2\pi fT}}{2} \left[e^{i\pi fT_+} \operatorname{sinc}(\pi f T_-) + e^{-i\pi fT_-} \operatorname{sinc}(\pi f T_+) \right] , \quad (12)$$

with short-hand notation $T_\pm \equiv T(1 \pm \hat{a} \cdot \hat{n})$.

3.2. Response of a simple Michelson interferometer

For continuous laser light with intrinsic angular frequency ω_0, the delay due to gravitational waves leads to a phase shift $\psi = \omega_0 \delta T$. Superposition of the two beams in a Michelson interferometer will produce a signal in the dark port proportional to the differential phase, which in the frequency domain can be written as

$$\tilde{\psi}(f) = \omega_0 T \left[F_+(\hat{n}, f) \tilde{h}_+(f) + F_\times(\hat{n}, f) \tilde{h}_\times(f) \right] , \quad (13)$$

where

$$F_A(\hat{n}, f) = \frac{1}{2} \left[D(\hat{a}, f)\, a^i a^j - D(\hat{b}, f)\, b^i b^j \right] .e^A_{ij}(\hat{n}) \quad (14)$$

In the limit $f = 0$, the Michelson response functions $F_A(\hat{n}, f)$ become the standard static antenna pattern functions (5).

3.3. Response of a Michelson interferometer with Fabry-Perot arm cavities

The presence of Fabry-Perot cavities in the interferometer arms adds further filtering of the signal. If the amplitude of the light incident on the cavity is A_0 and the phase of the light in one round-trip is $\psi(t)$, the multi-beam interference leads to

$$E(t) = t_1 A_0 \sum_{k=0}^{\infty} (r_1 r_2)^k e^{i\psi(t-2kT)} , \quad (15)$$

where $r_{1,2}$ and t_1 are the reflectivity and transmissivity of the cavity mirrors. Let the amplitude and the phase of this field be A and Ψ: $E = Ae^{i\Psi}$. Approximating $e^{i\psi} \approx 1 + i\psi$ in (15), and keeping only first order terms, we obtain that the amplitude of the field in the cavity is $A = t_1 A_0/(1 - r_1 r_2)$ and its phase is given by

$$\Psi(t) = (1 - r_1 r_2) \sum_{k=0}^{\infty} (r_1 r_2)^k \psi(t - 2kT) . \quad (16)$$

Equivalently, in the Fourier domain

$$\tilde{\Psi}(f) = H_{\rm FP}(f) \tilde{\psi}(f) , \qquad H_{\rm FP}(f) = \frac{1 - r_1 r_2}{1 - r_1 r_2 e^{-i4\pi fT}} . \quad (17)$$

Thus, the filtering properties of Fabry-Perot cavity can be taken into account by multiplying the Michelson response $F_A(\hat{n}, f)$ by the *direction-independent* transfer function $H_{\rm FP}(f)$:

$$G_A(\hat{n}, f) \equiv H_{\rm FP}(f) F_A(\hat{n}, f) . \quad (18)$$

Note that $H_{\rm FP}(f)$ can be rewritten as

$$H_{\rm FP}(f) = e^{i2\pi fT} \frac{\sinh(2\pi f_0 T)}{\sinh[2\pi f_0 T(1 + if/f_0)]} , \quad (19)$$

where f_0 is the lowest order pole, $f_0 \equiv -\ln(r_1 r_2)/(4\pi T)$. For the 4-km LIGO detectors, $f_0 \approx 86$ Hz. Figure 2 is a plot of the magnitude of the detector response functions $G_A(\hat{n}, f)$ at the free-spectral range (FSR) of the Fabry-Perot cavities for the LIGO 4-km interferometers, where $L = \lambda/2$ (corresponding to frequency $f = 37.5$ kHz). Note the presence of additional lobes and the factor of ≈ 6 reduction in overall amplitude relative to the static antenna pattern functions in Fig. 1

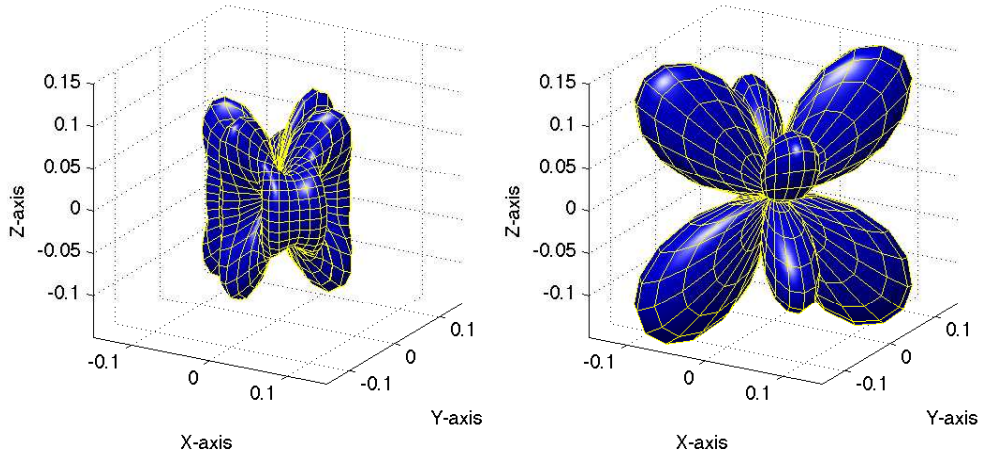

Figure 2. Detector response functions $|G_+(\hat{n}, f)|$ [left panel] and $|G_\times(\hat{n}, f)|$ [right panel] at the FSR ($f = 37.5$ kHz) of the Fabry-Perot cavities of the 4-km LIGO interferometers.

3.4. Long-wavelength approximation

At low frequencies ($f \ll f_{\rm FSR}$), it is common practice to approximate the detector response $G_A(\hat{n}, f)$ by the product

$$g_A(\hat{n}, f) \equiv H_{\rm pole}(f) F_A(\hat{n})\,, \qquad H_{\rm pole}(f) = \frac{1}{1 + if/f_0}\,, \tag{20}$$

where $F_A(\hat{n})$ are the static antenna pattern functions (5). Note that $g_A(\hat{n}, f)$ is a hybrid quantity consisting of the $f = 0$ limit of $F^A(\hat{n}, f)$, and the lowest-order approximation to $e^{-i2\pi fT} H_{\rm FP}(f)$. The usual practice of simply approximating the full Fabry-Perot response (18) with the single-pole transfer function (20) leads to errors in the phase as large as 10° at $f = 2$ kHz.

The magnitude of $g_A(\hat{n}, f)$ and the difference $G_A(\hat{n}, f) - g_A(\hat{n}, f)$ as functions of sky position at $f = 1024$ Hz are shown in Fig. 3. The magnitude of the long-wavelength detector response functions shown in the top two panels is down by a factor of ≈ 0.08 (relative to Fig. 1), due to the value of $H_{\rm pole}(f)$ at $f = 1024$ Hz. The maximum value of the correction terms shown in the bottom two panels is thus $\sim 1\%$ of the maximum long-wavelength values. This is about $10\times$ smaller than the nominal $\sim 10\%$ correction ($2\pi fT = 0.086$ at $f = 1024$ Hz), due to the angular dependence of the correction terms.

The effect of *first-order* corrections to the long-wavelength approximation for gravitational waves from a compact binary was recently analyzed by Baskaran and Grishchuk [4], for the case of a simple Michelson interferometer without the phase factor $e^{-i2\pi fT}$ in (12).

4. Effect of long-wavelength approximation on stochastic searches

The antenna pattern functions influence the response of a stochastic background search through the *overlap reduction function* [12]

$$\gamma(f) = \frac{5}{8\pi} \int_{S^2} d^2\Omega_{\hat{n}} F_{1A}^*(\hat{n}, f) F_{2A}(\hat{n}, f)\, e^{-i2\pi f \hat{n}\cdot(\vec{x}_1 - \vec{x}_2)/c}\,. \tag{21}$$

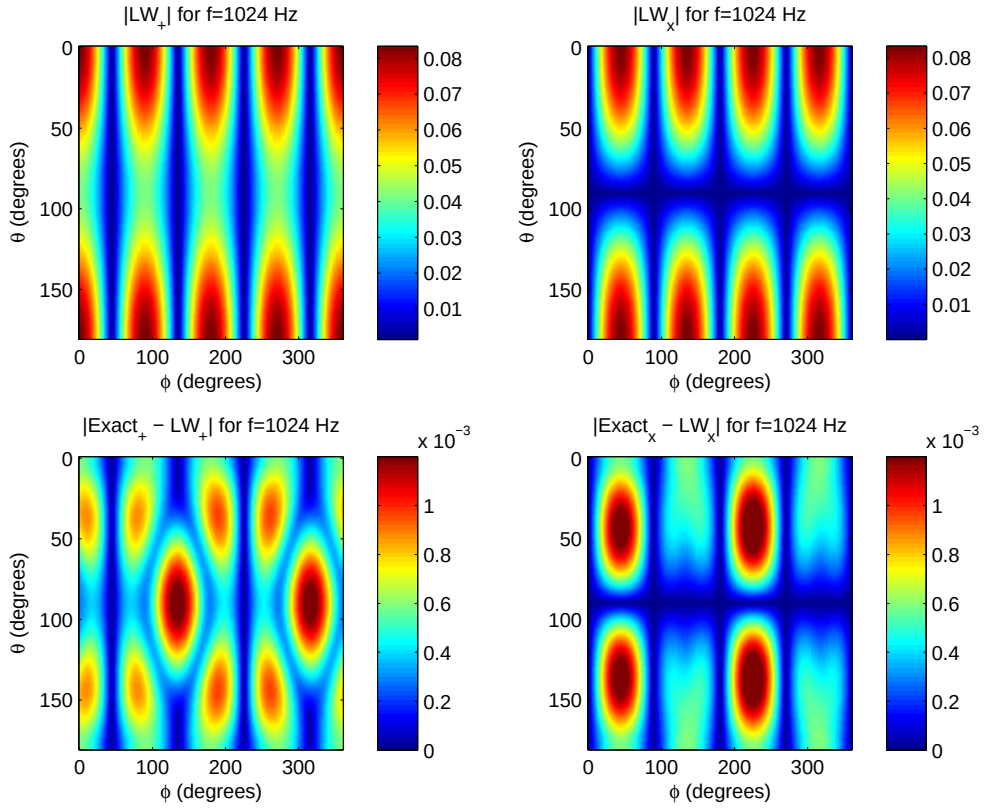

Figure 3. Magnitude of the long-wavelength detector response functions $|g_A(\hat{n}, f)|$ [top two panels], and the difference $|G_A(\hat{n}, f) - g_A(\hat{n}, f)|$ at $f = 1024$ Hz [bottom two panels]. Note that the maximum value of the difference is $\sim 1\%$ of the maximum long-wavelength values at this frequency.

The overlap reduction function specifies the reduction in sensitivity of a cross-correlation search for an isotropic stochastic background of gravitational waves due to the separation and relative mis-alignment of a pair of interferometers located at $\vec{x}_1$ and $\vec{x}_2$. A typical overlap reduction function is shown in Fig. 4 for the two 4-km-long inteferometers (H1 and L1) at the LIGO Hanford (LHO) and Livingston (LLO) Observatories, respectively.

Using the explicit forms of the exact and long-wavelength antenna pattern functions given in the previous section, it is possible to derive analytic expressions for the overlap reduction function not only for the long-wavelength limit, but also for the 1st-order correction [13]. The one stochastic search so far influenced by kHz frequencies was the LLO-ALLEGRO search [14]. Table 1 illustrates the corrections relevant at $f \approx 915\,\mathrm{Hz}$ due to the finite length of the L1 arms. Previous LHO-LLO correlation analyses have concentrated on frequencies $f \lesssim 300\,\mathrm{Hz}$, but inclusion of the 3-km long Virgo interferometer (V1) in LIGO's 5th science run (S5) has added interest in frequencies around 1 kHz. A typical measure of the impact of corrections to the long-wavelength approximation is the fractional change in the stastical one-sigma

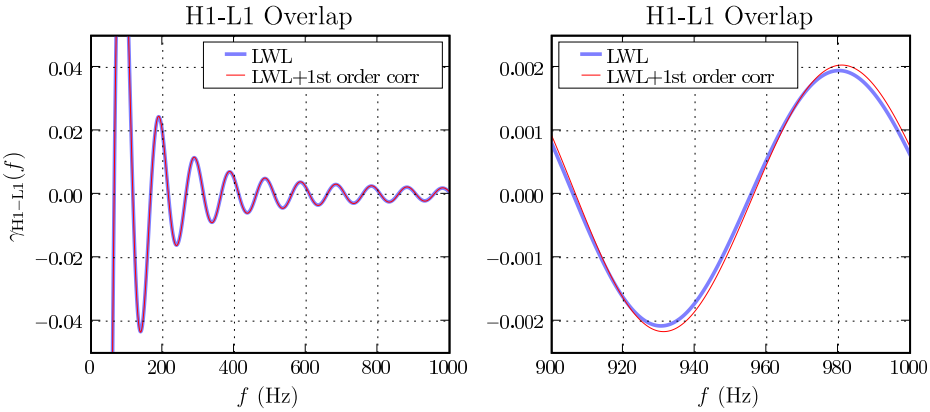

Figure 4. Overlap reduction function for the two 4-km-long LIGO interferometers H1 and L1. The standard long-wavelength form used in most ground-based analyses is shown, along with a version including 1st-order corrections.

Table 1. Impact of 1st-order corrections on LLO-ALLEGRO search. The corrections are less than 1%, except for the null orientation. The upper limits in [14] are not affected to the stated precision by these corrections.

	$\gamma^{\mathrm{LW}}(f)$	$\delta\gamma(f)$	$\delta\gamma(f)/\gamma^{\mathrm{LW}}(f)$
XARM	0.95333	0.00298	0.00313
YARM	−0.89466	−0.00167	0.00187
NULL	0.03181	−0.00061	−0.01914

Table 2. Impact of 1st-order corrections on error bars for pairs of interferometers. The numbers in the table are $\delta\sigma/\sigma^{\mathrm{LW}}$, calculated assuming a white stochastic backgrounds across the band shown, using the nominal design sensitivities of the instruments. The 4% correction for H1-L1 at 1 kHz is comparable to the current calibration uncertainties for these searches.

	H1-L1	H1-V1	L1-V1
$50-150\,\mathrm{Hz}$	-1.9×10^{-3}	1.9×10^{-4}	2.5×10^{-4}
$900-1000\,\mathrm{Hz}$	-4.2×10^{-2}	8.9×10^{-4}	1.1×10^{-3}

error bar σ:

$$\frac{\delta\sigma}{\sigma^{\mathrm{LW}}} = -\left(\int_{f_{\mathrm{min}}}^{f_{\mathrm{max}}} df\,\frac{\delta\gamma(f)\,\gamma^{\mathrm{LW}}(f)}{P_1(f)\,P_2(f)}\right)\Bigg/\left(\int_{f_{\mathrm{min}}}^{f_{\mathrm{max}}} df\,\frac{[\gamma^{\mathrm{LW}}(f)]^2}{P_1(f)\,P_2(f)}\right) \quad (22)$$

This contribution is less than 1% at frequencies considered in previous searches, and for H1-V1 and L1-V1 pairs around 1 kHz. But for the H1-L1 correlation around 1 kHz, the effect is 4% as shown in Table 2, comparable to the current calibration uncertainties for these searches.

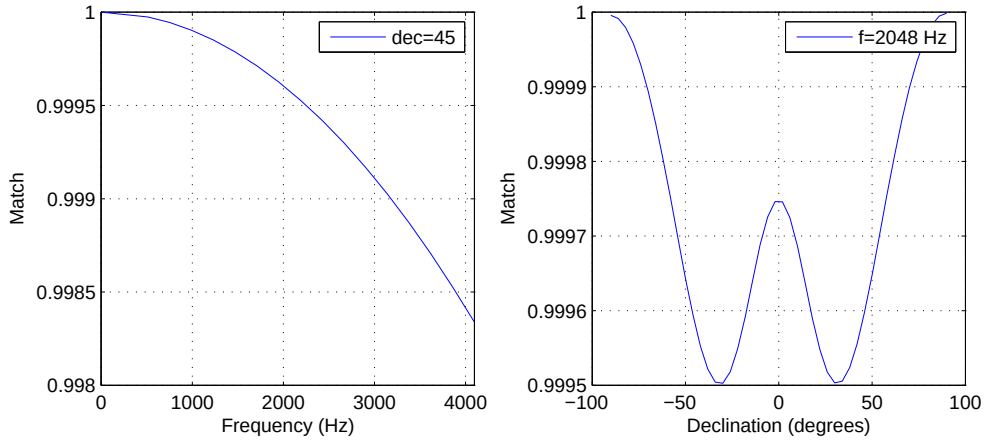

Figure 5. Fraction of maximum available SNR (i.e., match) as a function of frequency for fixed source declination (dec = 45°) [left panel], and as a function of source declination for fixed gravitational-wave frequency (f = 2048 Hz) [right panel].

5. Effect of long-wavelength approximation on searches for periodic gravitational waves

The heterodyned gravitational-wave signal for an isolated pulsar with known gravitational-wave frequency f and position in the sky $\hat{n}$ is given by [15]:

$$y(t) = \frac{1}{4}G_+(\hat{n}, f; t)h_0(1+\cos^2\iota)e^{i\phi_0} - \frac{i}{2}G_\times(\hat{n}, f; t)h_0\cos\iota\, e^{i\phi_0} \quad (23)$$

where h_0 is the amplitude, ι the inclination angle, and ϕ_0 the initial phase of the incident gravitational wave. The (slowly-varying) time-dependence in the antenna pattern functions comes from the Earth's sidereal rotational motion. (The unit vectors $\hat{a}$, $\hat{b}$, which point along the detector arms, rotate with the Earth and are thus time-dependent in equatorial coordinates.)

To assess the effect of using the long-wavelength approximation on a known pulsar search, we calculate the *match* between the signals y_1, y_2 defined by the exact and long-wavelength approximations to the detector response, respectively (cf. (18) and (20)):

$$\text{match} = \frac{\frac{1}{2}\int dt\,(y_1 y_2^* + y_1^* y_2)}{\sqrt{\int dt\,|y_1|^2}\sqrt{\int dt\,|y_2|^2}}\,. \quad (24)$$

The time integration is over 1 sidereal day. Note that (1−match) is the reduction in SNR that results from using the long-wavelength antenna pattern functions instead of the exact ones. Figure 5 shows: (a) the match versus frequency for fixed source declination (dec = 45°), and (b) the match versus declination for fixed gravitational-wave frequency (f = 2048 Hz) for the simple case where ψ, ι, and ϕ_0 are assumed to be known with values $\psi = 0$, $\iota = 0$, and $\phi_0 = 0$. This corresponds to a *circularly-polarised* gravitational wave. The detector arms $\hat{a}$, $\hat{b}$ were taken to be that of 4km LHO interferometer. Note that maximum reduction in SNR is much less than 1% for all directions on the sky and for gravitational-wave frequencies up to 4 kHz. Although this

is a highly-simplified example, it should be representative of the size of the systematic errors introduced by the long-wavelength approximation for periodic gravitational waves from known pulsars.

6. Summary

We have shown that for frequencies of order 1 kHz, the effect of corrections to the long-wavelength approximation are *negligible* for the isotropic stochastic and periodic gravitational-wave searches performed so far, typically being much less than 1%. However, for the planned LHO-LLO cross-correlation search for an isotropic stochastic background around 1 kHz, use of the long-wavelength approximation would introduce a systematic error of approximately 4% (see Table 2).

The presence of Fabry-Perot cavities in the interferometer arms gives us *another* frequency band to search for gravitational waves. For the 4-km LIGO interferometers this is approximately a 200-Hz peak centered at the FSR ($f = 37.5$ kHz). Enhanced sensitivity of the detectors (only a factor of 5-8 less than at DC) motivated installation of high-sampling rate (262 kHz) digitizers at both LIGO sites to produce Fast AS-Q data for searches of gravitational-wave signals at the FSR. Efforts to analyze the data from the Fast AS-Q channel during the 4th and 5th LIGO science runs are underway at the University of Rochester (for stochastic searches) [16] and LHO (for bursts) [17, 18]. The exact expressions for the detector response functions are a must for these searches.

Acknowledgments

The authors would like to acknowledge conversations with C Cutler, L Grishchuk, D Khurana, G Mendell, R Prix, R Savage, and G Woan. This work was supported by the Max-Planck-Society and the German Aerospace Center (DLR), and NSF grant PHY-0555842 awarded to The University of Texas at Brownsville. This paper has been assigned LIGO Document Number LIGO-P080036-00-Z.

References

[1] Barish B C and Weiss R 1999 *Physics Today* **52** 44–50
[2] Bradaschia C *et al.* 1990 *Nuclear Instruments and Methods in Physics Research A* **289** 518–525
[3] Willke B *et al.* 2002 *Class. Quantum Grav.* **19** 1377
[4] Baskaran D and Grishchuk L P 2004 *Class. Quantum Grav.* **21** 4041
[5] Schutz B F and Tinto M 1987 *Mon. Not. R. Astr. Soc.* **224** 131
[6] Gürsel Y, Linsay P, Spero R, Saulson P, Whitcomb S and Weiss R 1984 in *A Study of a Long Baseline Gravitational Wave Antenna System* (National Science Foundation Report)
[7] Sigg D 1997 Strain calibration in LIGO. LIGO Technical Report T970101-B
[8] Rakhmanov M 2006 Response of LIGO 4-km interferometers to gravitational waves at high frequencies and in the vicinity of the FSR (37.5 kHz). LIGO Technical Report T060237
[9] Schilling R 1997 *Class. Quantum Grav.* **14** 1513
[10] Larson S L, Hiscock W A and Hellings R W 2000 *Phys. Rev. D* **62** 062001
[11] Cornish N J and Rubbo L J 2003 *Phys. Rev. D* **67** 022001
[12] Flanagan É É 1993 *Phys. Rev. D* **48** 2389
[13] Whelan J T 2007 Higher-frequency corrections to stochastic formulae. LIGO Technical Report T070172-00-Z
[14] Abbott B *et al.* 2007 *Phys. Rev. D* **76** 022001
[15] Dupuis R J and Woan G 2005 *Phys. Rev. D* **72** 102002
[16] Forrest C, Fricke T, Giampanis S and Melissinos A 2007 Search for a diurnal variation of the power detected at the FSR frequency. LIGO Technical Report T070228-00-Z

[17] Savage R L *et al.* 2006 LIGO high-frequency response to length- and gw-induced optical path length variations. LIGO Technical Report G060667
[18] Parker J 2007 Development of a high-frequency burst analysis pipeline. LIGO Technical Report T070037-00-W